IEEE Access
Multidisciplinary | Rapid Review | Open Access Journal

Received December 2, 2018, accepted December 12, 2018, date of publication December 18, 2018,
date of current version January 11, 2019.

Digital Object Identifier 10.1109/ACCESS.2018.2887296

Low-Light Image Enhancement by Principal Component Analysis

STEFFI AGINO PRIYANKA[1], YUAN-KAI WANG[2], AND SHIH-YU HUANG[3]
[1]Graduate Institute of Applied Science and Engineering, Fu Jen Catholic University, New Taipei City 24205, Taiwan
[2]Department of Electrical Engineering, Fu Jen Catholic University, New Taipei City 24205, Taiwan
[3]Department of Information and Communication Engineering, Ming Chuan University, Taoyuan 333, Taiwan

Corresponding author: Yuan-Kai Wang (ykwang@fju.edu.tw)

This work was supported by the Ministry of Science and Technology, Taiwan.

ABSTRACT Under extreme low-lighting conditions, images have low contrast, low brightness, and high noise. In this paper, we propose a principal component analysis framework to enhance low-light-level images with decomposed luminance–chrominance components. A multi-scale retinex-based adaptive filter is developed for the luminance component to enhance contrast and brightness significantly. Noise is attenuated by a proposed collaborative filtering employed to both the luminance and chrominance components that reveal every finest detail by preserving the unique features in the image. To evaluate the effectiveness of the proposed algorithm, a simulation model is proposed to generate nighttime images for various levels of contrast and noise. The proposed algorithm can process a wide range of images without introducing ghosting and halo artifacts. The quantitative performance of the algorithm is measured in terms of both full-reference and blind performance metrics. It shows that the proposed method delivers state-of-the-art performance both in terms of objective criteria and visual quality compared to the existing methods.

INDEX TERMS Contrast enhancement, denoising, principal component analysis.

I. INTRODUCTION

Recently the enhancement of low-light image has attracted broad interests tremendously, because of increasing demand of night-time imaging to visualize extensive activities of interest taking place in the dark, that is required by numerous applications including video surveillance, computational photography, and medical imaging. Over the last several decades, there have been substantial improvements in modern digital cameras including resolution and sensitivity to obtain images with optimum contrast. Despite these improvements, quality of images in low-light conditions is still limited. Low-light images have low illumination, low contrast and high noise. Low-light images have low signal-to-noise ratio which means high noise. Enhancing the contrast of night images is very vital to monitor the objects or activities of the scene clearly.

Several contrast enhancement techniques have been introduced to obtain clear night images with least noise. However, it remains a challenging task to enhance the contrast while keeping the noise minimal. Noise increases when the illumination is increased, but on the other hand, reducing the noise results in low brightness and contrast [1]. Many researchers have attempted to obtain clear night images by increasing the contrast. However, night images have both low contrast and high Poisson noise [2]. Some researchers focused on denoising the additive white Gaussian noise, whereas night images contain Poisson noise. Treating the Poisson noise while increasing the contrast remains a challenge.

Enhancing the contrast alone increases the brightness and luminance of the image, thereby making the image visible to the human eye. Syed and Justin [3] modified traditional histogram equalization to maintain the color information. Each color channel is enhanced separately by multiplying the ratio of the enhanced luminance to original luminance. However, the enhancement is restricted due to the loss of information in the frames. Yamasaki *et al*. [4] decomposed the image into illuminance and reflectance components to reproduce a natural image. The illuminance component was treated by a denighting algorithm. But this technique introduced ghosting artifacts. Li *et al*. [5] used algorithms like tone mapping, histogram equalization, histogram stretching, and gamma correction to recover visual information in low light images and videos. Although this approach produced visually pleasing enhancement results, it still needs information from successive frames in order to apply for a single image. Xiang *et al*. [6] implemented a de-haze algorithm to

the inverted input image in order to amplify the intensity. It introduced halo artifacts along with enhanced contrast. Rivera *et al*. [7] used an adaptive transformation function specialized for low-light images. This method enhanced the contrast of dark images, but could not recover information from shadowed or dark areas that had near-black intensities. A retinex model is used to process color images. This method enhanced high-frequency information such as edges and corners. However, they could not effectively avoid uneven contrast [8]. Meylan and Susstrunk [9] proposed a center–surround retinex based adaptive filter for high dynamic range (HDR) rendering. However, difficulties arose when the recorded images suffered from the loss in clarity of details and color as the distance from lighting source increased. All these methods successfully enhanced the contrast but amplified the noise. Noise amplification results in significant degradation of image quality. Therefore, simultaneous contrast enhancement and denoising of images remain a major challenge.

Denoising technique processes noisy images to remove the unwanted noise and restores the original image for obtaining useful information. Several algorithms have been proposed to reduce noise in spatial and spatiotemporal domains. Bennett and McMillan [10] presented an adaptive spatiotemporal accumulation filter for reducing noise in low dynamic range videos in addition to tone mapping. Kim *et al*. [11] used the spatiotemporal filter to suppress noise in the low-light-level video. However, strong denoising causes over-smoothing and blurring effect. Paris *et al*. [12] used a bilateral filter to smooth noisy images while preserving the edges. Nonetheless, direct implementation of bilateral filter does not achieve real-time performance on high definition content. It also leads to over-smoothing and edge sharpening. Dong *et al*. [13] captured multiple images and calculated the mean to remove noise. Each pixel was obtained as a weighted average of pixels centered at regions that are similar to the region centered at the estimated pixel. However, this method is impractical for a single image. Dong *et al*. [14] proposed a typical joint distribution wavelet method for removing noise from digital images. Although the wavelet-based method is popular and dominant in denoising, it introduces ringing artifacts, additional edges or structures in the denoised image. Talebi and Milanfar [15] pre-filtered the noisy image by using the bilateral filter. Eigenvectors were approximated by using Nystrom and Sinkhorn approximation. Truncated and iterative filters were used to get the denoised image. This process could be prolonged and complicated if the eigenvalues were to be estimated for the full image. BM3D [16] processes a noisy image in a blockwise manner forming a 3D array and filtered by 3D transform-domain shrinkage. References [9] and [16] proved to be a very promising method for contrast enhancement and denoising.

For night image enhancement, both contrast and noise have to be processed simultaneously. Enhancing the contrast alone increases the visibility of the images but amplifies the noise which can conceal important information. On the other hand, denoising alone removes the noise and restores the original image by preserving useful information, but results in low visibility. Recently a decomposition approach which extracts independent components of low-light images for separate processing of contrast and noise have arisen. Bright channel [17], bilateral filtering [18], wavelet transform [19], total variation [20] and sparse representation [21] have been applied to extract two or several components, which can be base-detail components, low-high frequency components, and space-time components. Contrast and noise can be dealt with separately in different components. However, components in those decomposition methods are not orthogonal. Therefore, the processing of contrast and noise in the components are correlated with side effects. Fu *et al.* [22] proposed a fusion-based (FB) method to adjust the illumination by fusing multiple derivations of the initially estimated illumination map. Its performance is promising but loses the realism of regions with rich textures due to the blindness of illumination structure.

Besides contrast enhancement and denoising, the evaluation of these algorithms is also important. The proposed algorithm has to be evaluated and compared with the state-of-the-art. Currently algorithms are evaluated from two aspects: qualitative and quantitative [23]. Image quality assessment (IQA) is significant in image processing due to its assistance in the development of enhancement [24] and denoising. Existing IQA techniques are devout to compression, transmission error, noise and blurring artifacts [25]. Based on the accessibility of reference source images to be compared with during the experiments, IQA approaches can be classified into three categories: full- reference (FR), reduced reference (RR), and no-reference (NR)/ blind metrics. FR algorithms are provided with the original undistorted visual stimulus along with distorted stimulus whose quality is to be assessed e.g., peak signal-to-noise ratio (PSNR) and structural similarity index (SSIM) [26]. RR methods work under the situation that the image can be partly available to assist in IQA tasks [27]. Finally, in blind metric method the original image is unavailable or the algorithm is provided only with distorted stimulus. e.g., blind pseudo reference image [28], NR image quality metric for contrast distortion (NIQMC) [29], and blind image quality measure of enhanced images (BIQME) [30], blind multiple pseudo reference image [31].

In our previous work [32], we introduced an image enhancement algorithm that enhances the contrast and a bilateral filter is used in the RGB channel for denoising, which results in over smoothing of images. But, in this paper, we propose a retinex based adaptive filter for Contrast Enhancement and Denoising (CED) algorithm by Principal Component Analysis (PCA) transform. Collaborative filtering is used to reduce the Poisson noise effectively and enhance the brightness and contrast of an image.

PCA is a method of discovering the dependencies in data and used for data dimension reduction, compression, and correlation. It transforms many possibly correlated variables

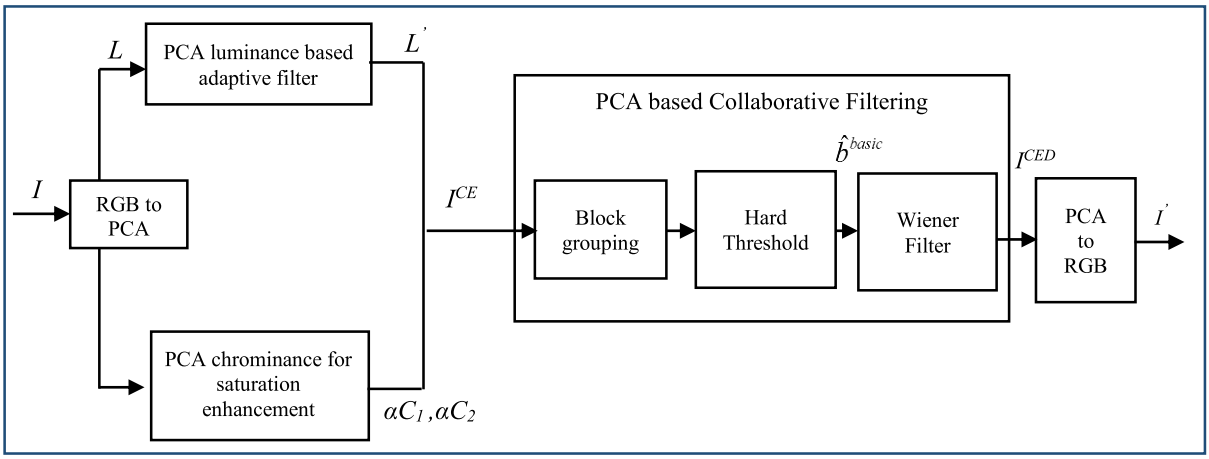

FIGURE 1. Flow of CED algorithm.

into a smaller number of new independent variables known as principal components [33]. It is used in image processing for image color reduction and determination of selected object orientation. In our work, the image is first transformed into luminance-chrominance components by using PCA. Global and local tone mapping algorithms are developed to eliminate halo and ghosting artifacts that were encountered in previously developed methods. Retinex based adaptive filter and collaborative filters are devised for contrast enhancement and denoising respectively.

A simulation model is also proposed to evaluate the effectiveness of the proposed CED algorithm for various levels of noise and contrast using generated images. Real images cannot be used to validate the effectiveness of the proposed algorithm for various levels of noise and contrast because in real night images the level of noise and contrast cannot be measured. Experimental results of this simulation model demonstrate that the proposed CED algorithm produces optimum contrast enhancement without artifacts and eliminates Poisson noise in night images.

The paper is organized as follows: The developed CED algorithm is described in section II and the proposed simulation model in section III. Experimental results and comparison with some existing algorithms are presented in section IV and relevant conclusions in section V.

II. CED ALGORITHM

Enhancing the contrast while keeping the noise minimal remains a challenge because noise increases when the illumination is increased. On the other hand, reducing the noise results in low brightness and low-contrast. Denoising followed by contrast enhancement introduces ringing artifacts. So, in our work the image is first enhanced by contrast followed by denoising to obtain better results. The luminance and chrominance components are processed in parallel. Because in color images, detail perception of each pixel is obtained from the luminance component since human vision system is not well suited to detect structures defined by varying chrominance values. Applying an enhancement technique to individual RGB channels boosts noise, since enhanced noisy chrominance edges generates more noise in the luminance. The contrast enhanced noisy image is first grouped by block matching to find the blocks that are similar to reference one and stack them together to form a 3D array. Collaborative filtering by hard thresholding is performed at the initial step because the noise in the initial step is assumed to be significantly attenuated. In the second step, Wiener filtering is applied to obtain the final denoised image.

A global framework of the proposed CED algorithm is shown in Fig. 1. It includes both contrast enhancement and denoising stages. The input RGB image I is decomposed into luminance and chrominance components through PCA. An adaptive filter is applied to the luminance component to obtain enhanced luminance L'. Saturation enhanced chrominance and L' are combined to obtain the contrast-enhanced image I^{CE} in PCA domain for denoising. I^{CE} is denoised through block grouping in PCA domain through effective filtering by hard thresholding to obtain the basic estimate $\hat{b}^{basic}$. The $\hat{b}^{basic}$ is then grouped and filtered by Wiener filter to acquire I^{CED}. Inverse PCA transform is applied to I^{CED} to obtain the output image.

A. CONTRAST ENHANCEMENT

The input RGB image I is decomposed into luminance and chrominance components and processed in parallel. PCA luminance component is obtained from the first principal component of I. Tone mapping algorithm is implemented to the PCA luminance to obtain globally corrected luminance. Multi-scale retinex based adaptive filter is applied in log domain to the globally corrected luminance. L' is acquired after histogram modification is pertained to scale the luminance of the image to circumvent over enhancement. Simultaneously, in the chrominance channels a tone mapping algorithm is implemented to the input image I for

global compression, and the logarithm is applied to this globally corrected image. The globally corrected image is then transformed to obtain luminance – chrominance components through PCA transform. Weighting factor α is introduced in chrominance components to compensate for the loss of saturation. Enhanced chrominance and L' are combined to obtain I^{CE}.

PCA luminance-chrominance channels are obtained by converting the I using PCA transform. PCA of I can be described as a transform of a given set of n pixels with the same length M formed in n-dimensional vector $X = [x_1, x_2, \ldots x_n]$, $x_i = (r_i, g_i, b_i)^{\mathrm{T}}$, into a set of vectors $Y = [y_1, y_2, \ldots y_n]$, $y_i = (L, C_{1i}, C_{2i})^{\mathrm{T}}$, according to the equation,

$$Y_i = A\,(x_i - \bar{m}) \tag{1}$$

where $\bar{m}$ is a mean vector and A is a transform matrix obtained by Σ_x. Each row of the vector x_i consists of M values belonging to one input. The mean vector $\bar{m}$ of all pixels is given as follows,

$$\bar{m} = E\{x\} = \frac{1}{M}\sum_{i=1}^{M} x_i \tag{2}$$

The luminance component of I from PCA are $L = [l_1, l_2, \ldots l_n]$, and chrominance components of I from PCA are $C_1 = [c_{11}, c_{12}, \ldots c_{1n}]$ and $C_2 = [c_{21}, c_{22}, \ldots c_{2n}]$. Covariance matrix Σ_x is defined as follows:

$$\begin{aligned}\Sigma_x &= E\left\{(x - \bar{m})\,(x - \bar{m})^T\right\} \\ &= \frac{1}{M}\sum_{i=1}^{M} x_i x_i^T - \bar{m}\bar{m}^T\end{aligned} \tag{3}$$

The size of Σ_x is 3×3 and the diagonal elements $\Sigma_x(j, j)$, $1 \le j \le 3$ are the variances of red, green and blue channels individually. The non-diagonal elements $\Sigma_x(j, k)$ are the covariances between two channels.

To perform PCA, it is necessary to find the eigenvalues λ and eigenvectors e of Σ_x. The three eigenvectors e_j, $1 \le j \le 3$, are arranged in decreasing order following the eigenvalues λ_j. The transform matrix $A = [\lambda_1, \lambda_2, \lambda_3]^{\mathrm{T}}$ is obtained by combining the sorted eigenvalues and its value is replaced in (1). The luminance chrominance components are decomposed from (1) and are given by the following equation,

$$\begin{aligned}L &= \lambda_1^T\,(x_i - \bar{m}) \\ C_{1i} &= \lambda_2^T\,(x_i - \bar{m}) \\ C_{2i} &= \lambda_3^T\,(x_i - \bar{m})\end{aligned} \tag{4}$$

The matrix theory implies that the image obtained by reconstruction with matrix λ_1^T (largest eigenvalue) contains the majority of information which has the maximum contrast. The luminance L is given by the first principal component of I, which lies in the range [0, 1].

The PCA luminance and chrominance channels are enhanced separately but simultaneously. The global tone mapping function is approximated by the power function [9],

$$\Re = (L)^{1/\gamma} \tag{5}$$

$$\frac{1}{\gamma} = \left(1, \frac{1}{6}\bar{L} + \frac{2}{3}\right) \tag{6}$$

where the value of $\frac{1}{\gamma}$ is a linear function of the average luminance and lies in the range $[\varepsilon, 1]$. The coefficient of the linear function is defined experimentally as follows: for the image with high or average brightness, $\frac{1}{\gamma} = 1$ is assigned. If the average luminance decreases, the exponent value also decreases, resulting in an increase in the sensitivity for dark areas. The average luminance value $\bar{L}$ is computed by taking the average of log encoded pixels.

$$\bar{L} = \frac{\sum_{(x,y)\in L} \log\left(L\,(x, y)\right)}{M} \tag{7}$$

where M is the number of pixels and (x, y) is the pixel coordinates in L. Tone mapping algorithm applied to the luminance component improves the brightness and contrast.

After global tone mapping, local processing is performed by an adaptive multi-scale retinex (MSR) to compute a new value for each pixel by taking the difference between the log-encoded treated pixel and log encoded value of the mask. The MSR combines several single-scale retinex outputs to produce a single output image, which has good dynamic range compression, color constancy and tonal rendition [34]. The MSR is applied to the luminance channel to increase the contrast and brightness of the image. Therefore, the new luminance $\bar{\Re}(x, y)$ after applying MSR is described by the equation,

$$\bar{\Re}(x, y) = \sum_i W_k\left[\log\left(\Re(x, y)\right) - \beta(x, y)\log(mask(x, y))\right] \tag{8}$$

$$\beta\,(x, y) = 1 - \frac{1}{1 + e^{-7(\Re(x,y)-0.5)}} \tag{9}$$

To achieve adaptive local normalization, a weighting factor $\beta(x, y)$ is introduced. The weighting factor β maps the white pixels to white and the black pixels to black. *Mask* denotes weighted average of the treated pixel's surrounding area. The mask weights of high and low-intensity pixels are close to 0 and 1 respectively. The mask is computed specifically for each pixel using the equation,

$$mask\,(x, y) = \frac{\sum_{\theta=0}^{360}\sum_{r=0}^{r_{\max}} \Re\,(x + r\cos\theta, y + r\sin\theta)e^{r^2/\sigma_{\theta,r}^2}}{\sum_{\theta=0}^{360}\sum_{r=0}^{r_{\max}} e^{r^2/\sigma_{\theta,r}^2}} \tag{10}$$

where θ is the angle of the radial direction and r is the distance to the central pixel and $\sigma_{\theta,r}$ is given as follows:

$$\sigma_{\theta,r}^2 = \begin{cases}\sigma_\theta, & \text{no high - contrast edge - crossed} \\ \sigma_1, & \text{high - contrast edge - crossed}\end{cases} \tag{11}$$

The value of the mask at coordinates (x, y) is given by the weighted average of the surrounding pixels of the Gaussian function. An adaptive filter is used to minimize the tradeoff between the increase in local contrast and good rendition of the image. It prevents from halo artifacts and adapts to high contrast edges in the image. The spatial constant changes in accordance with high contrast image edges. Central pixel is chosen as the first pixel and masking is done by selecting one pixel after another in a radial manner. If an edge is crossed, $\sigma_{\theta,r}$ is given smaller value σ_1 otherwise, σ_0 is assigned. $\sigma_{\theta,r}$ is reset to its initial value σ_0 for each new radial direction.

To scale the luminance of the image, histogram modification [35] is implemented to reduce the over contrasted areas in the enhanced image. After histogram modification, histogram equalization [36] is accomplished to adjust the contrast of the image to avoid over enhancement problem. PCA chrominance is obtained after applying a tone-mapping algorithm from (6) to I and logarithm to the tone mapped image in the chrominance channels. The chrominance channels are weighted by a factor α to compensate for the loss of color saturation induced by enhanced luminance. Finally, the I^{CE} for denoising is obtained by combining saturation enhanced chrominance channels and L' (obtained after histogram modification and equalization).

$$I^{CE} = L' \times \alpha C_1 \times \alpha C_2 \tag{12}$$

B. DENOISING

Noise in low light images is usually caused by thermal noise in the camera's electronic circuitry. At low light levels, the gain of the image sensor in a camera is increased to boost the signal to an acceptable level. As a result, the noise is augmented. This noise is referred to as Poisson noise. Eliminating the Poisson noise in low light images is very essential to obtain useful information. In this work, the image is denoised in PCA transform domain through effective filtering in 3D transform domain (hard-thresholding and wiener filtering) by sliding window transform processing and block matching, which are stacked together to form a 3D array. The final estimate is obtained by the weighted average of all the overlapping block estimates. Denoising is a two-step algorithm where a basic estimate is produced by grouping and hard-thresholding. In the second step, basic estimate is used for grouping and Wiener filter is applied to obtain the final estimate. The final estimate is the denoised image which is then converted back to RGB color space by applying inverse PCA transform. The noisy image is modeled as

$$I^{CE}(x) = J(x) + N(x) \tag{13}$$

where I^{CE}, J and N are the contrast-enhanced noisy image, the noise-free image, Poisson noise and x is the 3D spatial coordinate that belongs to the image domain $X \subset \mathbb{Z}^3$.

Grouping is realized by similarity and block matching within the noisy image. The purpose of grouping is to collect similar d-dimensional fragments of a given signal into a $d+1$ dimensional data structure. A 3D array is formed by stacking

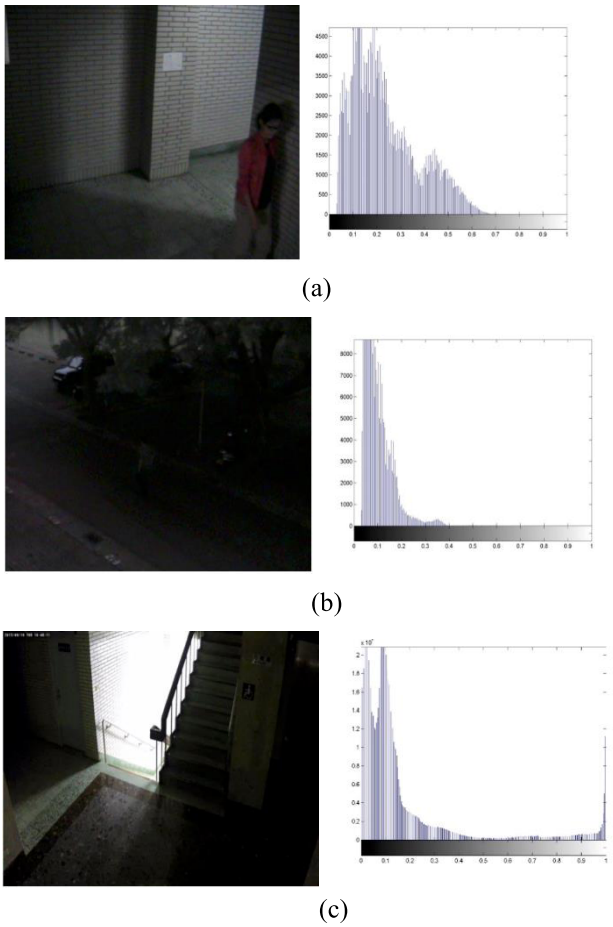

FIGURE 2. Classification of contrast levels. (a) LLL, (b) VLLL, (c) HDR.

grouped blocks located in the region I^{CE}. The inverse of the distance measure gives the similarity value between signal fragments. Smaller the distance, higher the similarity value. Grouping by matching is realized through finding similarity between reference and candidate signal fragments located at different spatial locations. The fragments are considered mutually similar and subsequently grouped if the distance from the reference one is smaller than the given threshold. With I_x^{CE}, we denote a block of size $N_1 \times N_1$ in I^{CE} where I_x^{CE} is located at x in I^{CE}. For noisy image I^{CE}, the block distance is calculated from the noisy blocks $I_{x_R}^{CE}$ and I_x^{CE} as

$$D^{noisy}\left(I_{x_R}^{CE}, I_x^{CE}\right) = \frac{\left\| I_{x_R}^{CE} - I_x^{CE} \right\|_2^2}{\left(B_1^{ht}\right)^2} \tag{14}$$

where $\|.\|_2$ denotes l^2 norm, $I_{x_R}^{CE}$ is the currently processed block (located at the current coordinate $x_R \in X$) and denominate it reference block and B_1^{ht} is the block size. Block matching (BM) using I_x^{CE} as a reference block, the result is the set H_x which contains the coordinates of the matched blocks.

$$H_x = BM\left(I_x^{CE}\right) \tag{15}$$

FIGURE 3. Enhancement results of the proposed algorithm. (a) - (d) Real night images of different scenes, (e) - (h) corresponding results.

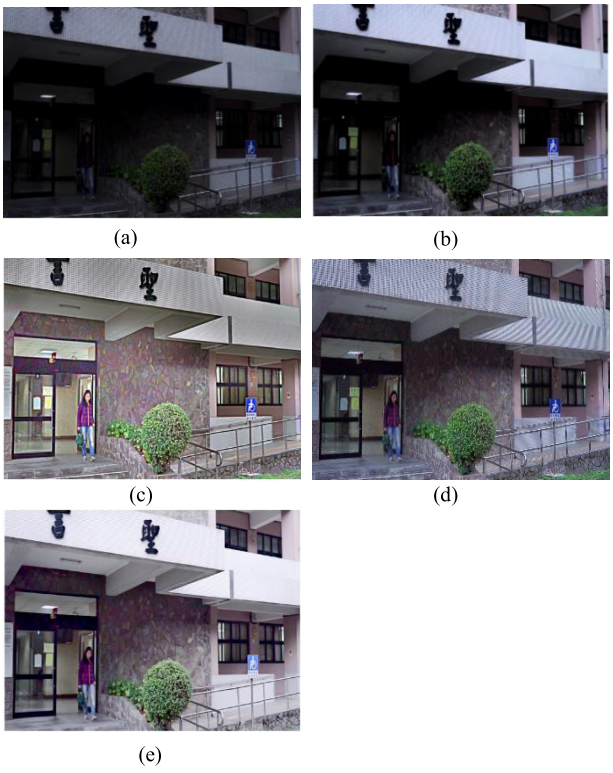

FIGURE 4. Comparative analysis of different algorithms with real night image. (a) Night image, (b) contrast pair, (c) P-retinex, (d) FB, and (e) CED.

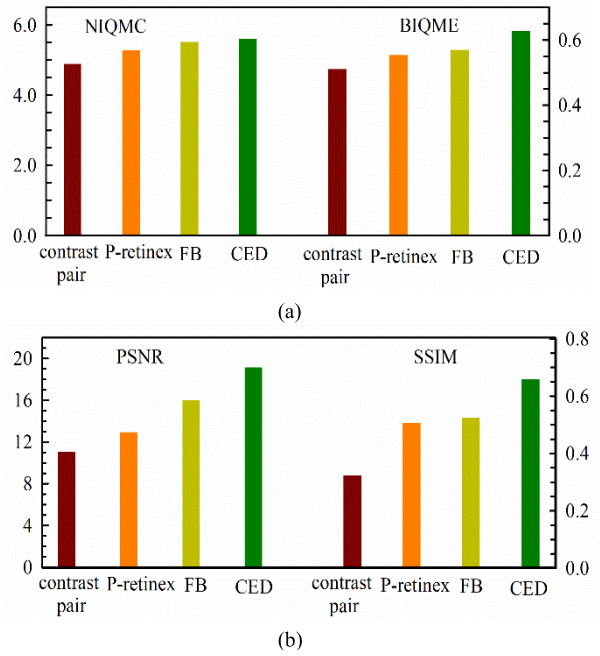

FIGURE 5. Comparing the average results of various real night images for different evaluation metrics. (a) Blind metric, (b) full-reference metric.

Noise attenuation is performed efficiently by collaborative filtering using 3D transform and shrinkage of transform spectrum.

To obtain the basic estimate, the noise is attenuated by applying hard thresholding shrinkage operator to the transform coefficients $\left(HT\left(T_{3D}\left(I_{H_x}^{CE}\right), \lambda_{3D\sigma}\right)\right)$. The coefficients are obtained by applying a 3D transform to each group to obtain the sparse representation of the signal,

$$\hat{Y}_{H_x} = T_{3D}^{-1}\left(HT\left(T_{3D}\left(I_{H_x}^{CE}\right), \lambda_{3D\sigma}\right)\right) \tag{16}$$

where $\hat{Y}_{H_x}$ is a group of block-wise estimates $\hat{Y}_{x'}^{x}, \forall x' \in H_x . I_{H_x}^{CE}$ denotes a group (i.e. a 3D array) formed by stacking together the blocks $I_x^{CE} \in H_x$, $\left(T_{3D}\left(I_{H_x}^{CE}\right)\right)$ is the spectrum of $I_{H_x}^{CE}$ using 3D linear transform T_{3D} which should have a

DC basis element (e.g. 3D-DCT, 3D-DFT, etc.) and $\lambda_{3D\sigma}$ is a fixed threshold parameter. The basic estimates $\hat{b}^{basic}$ are obtained by the inverse 3D transform of the filtered coefficients. The basic estimate is computed by aggregation of block-wise estimates $\hat{Y}^x_{x'}, \forall x' \in X_R$ and $\forall x' \in H_x$ using weighted averaging with weight,

$$W_H = \hat{Y}^x_{x'} = \frac{1}{\sigma^2 N_h(x)} W_{2D} \tag{17}$$

$$\hat{b}^{basic}_x(x) = \frac{\sum_{x_R \in X} \sum_{x_m \in H_x} \hat{Y}^x_x \hat{Y}_{H_x}(x)}{\sum_{x_R \in X} \sum_{x_m \in H_x} \hat{Y}^x_{x'} \chi x_m(x)}, \quad x \in X \tag{18}$$

where $N_h(x)$ is the number of non-zero coefficients retained after hard thresholding $T_{3D}(I^{CE}_{H_x})$ and W_{2D} is a 2D Kaiser window of size $N_1 \times N_1$.

In the second step, the obtained basic estimate $\hat{b}^{basic}$ is used for grouping and Wiener filter is applied to obtain the final estimate $\hat{b}^{final}$. In this case, the denoising can be improved because the noise in $\hat{b}^{basic}$ is assumed to be significantly attenuated. The Wiener filter shrinkage operator is applied and the same procedure is followed.

$$W_x = BM\left(\hat{b}^{basic}_x\right) \tag{19}$$

$$\hat{Y}_{W_x} = T^{-1}_{3D}\left(T_{3D}\left(I^{CE}_{W_x}\right) \frac{\left(T_{3D}\left(\hat{b}^{basic}_{W_x}\right)\right)^2}{\left(T_{3D}\left(\hat{b}^{basic}_{W_x}\right)\right)^2 + \sigma^2}\right) \tag{20}$$

Wiener shrinkage coefficients are defined from the basic estimate of 3D transform coefficients. The Inverse transform $\left(T^{-1}_{3D}\right)$ is applied to produce the block-wise estimates located at matched locations. To compute the final estimates $\hat{b}^{final}$ of the image, block wise estimates are aggregated by a weighted average of the obtained block wise estimates.

$$W_W = \hat{Y}^x_{x'} = \sigma^{-2} \left\| \frac{\left[T_{3D}(\hat{b}^{basic}_{W_x})\right]}{\left[T_{3D}(\hat{b}^{basic}_{W_x})\right]^2 + \sigma^2} \right\|^{-2}_2 W_{2D} \tag{21}$$

$$I^{CED} = \hat{b}^{final}_x(x) = \frac{\sum_{x_R \in X} \sum_{x_m \in W_x} \hat{Y}^x_{x'} \hat{Y}_{W_x}(x)}{\sum_{x_R \in X} \sum_{x_m \in W_x} \hat{Y}^x_{x'} \chi x_m(x)}, x \in X \tag{22}$$

where $\chi x_m : X \to \{0, 1\}$ is the characteristic function of the square support of a block located at $x_m \in X$. The final estimate $\hat{b}^{final}$ is the denoised image I^{CED} in PCA domain. The final denoised or the output image I' is obtained by transforming I^{CED} to RGB color space by applying inverse PCA transform.

III. NIGHT IMAGE SIMULATION MODEL

Night image simulation model is imperative to validate the effectiveness of the proposed algorithm. Real night images cannot be used to validate the effectiveness of the proposed algorithm for various levels of noise and contrast because in real night images the level of noise and contrast cannot be measured. To do so, first night images are classified into three levels based on the contrast: low light level (LLL), very low light level (VLLL) and HDR images. In LLL, the image is completely dark and the objects in the scene are partially recognizable by the human eye. In VLLL, the overall image is dark and objects in the scene are unrecognizable by the human eye. HDR images have both brightest and darkest areas due to the photosensitive element that lies in saturated and unsaturated conditions. In LLL and VLLL images, dark areas are due to the photosensitive element in an unsaturated state. Fig. 2 shows the LLL, VLLL and HDR images with their respective histograms. For LLL and VLLL, night images are simulated from day image at different contrast levels by first, decreasing the luminance d and then, histogram compression α. The value of d is calculated from the cumulative distribution function (CDF) with respect to threshold t. The simulation is represented by the equation,

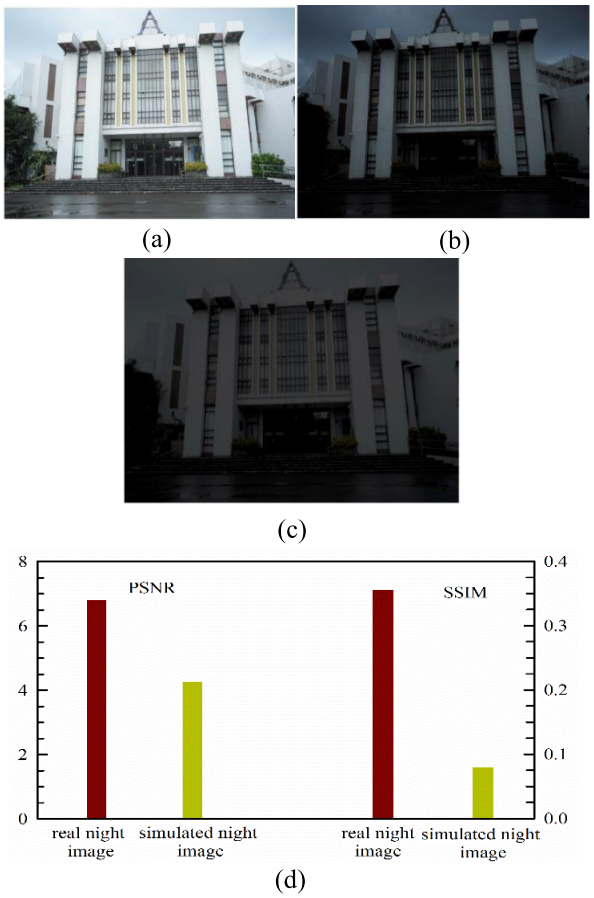

FIGURE 6. Verification of simulation model. (a) Source image, (b) real night image, (c) simulated night image, and (d) quantitative analysis.

$$f(x) = \alpha\left(\max\left(x - d, 0\right)\right), \quad d = \min\left\{i \,|cdf(i) \geq t\right\} \tag{23}$$

Similarly, HDR image is simulated by luminance saturation d and histogram stretching α using the following equation,

$$f(x) = \alpha \min\left(\max\left(x - d_{low}, 0\right), d_{high} - d_{low}\right) \tag{24}$$

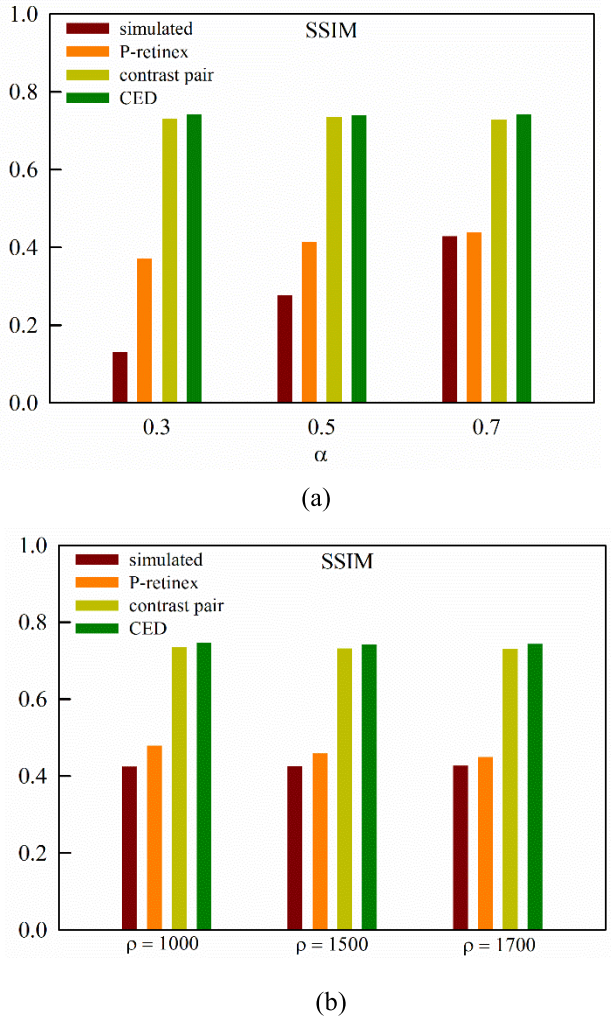

FIGURE 7. Comparisons of algorithms. (a) Various levels of contrast, (b) various levels of noise.

where $d_{low} = \min\{i \,|cdf(i) \geq t_{low}\}$,

$$d_{high} = \max\left\{i \,|cdf(i) \leq 1 - t_{high}\right\},$$
$$0 \leq t_{low}, \quad t_{high} \leq 1, \; t_{low} + t_{high} \leq 1 \tag{25}$$

Poisson noise in the night image is simulated by using the equation,

$$g(z) = \frac{e^{-\rho}\rho^{f(z)}}{f(z)!} \tag{26}$$

where $g(z)$, $f(z)$ and ρ are the noisy image, the original image and expected number of photos per unit interval respectively.

IV. EXPERIMENTAL RESULTS

In this section, experiments were conducted with real night images under various scenes for different lighting conditions with and without human objects for subjective and objective evaluations. The proposed algorithm is compared

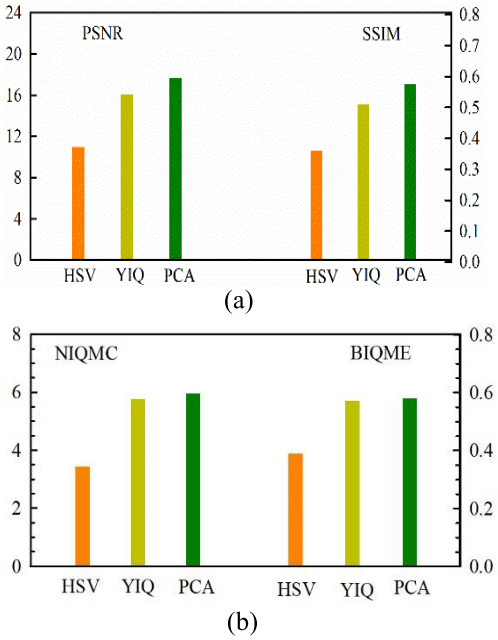

FIGURE 8. Analysis of different color transforms for real night images. (a) FR metrics, (b) blind metric.

with other existing contrast enhancement and denoising algorithms for various levels of contrast, noise, and their results are compared. The contrast and denoise analysis are done individually utilizing generated image because the real night image contains both noise and low contrast and it is impossible to analyze separately. our simulation model is verified by comparing real and generated night image and the results are analyzed using FR performance metrics. Results of simulation model show that the generated image is analogous to real night image which can be used to validate the effectiveness of the proposed algorithm. Experiments are done to analyze PCA and it is compared with other color transforms to justify that PCA performs better in comparison with other color transforms. For all the experiments, images were captured using SONY ILCE-7 digital camera with a resolution 1024×768.

A. COMPARATIVE ANALYSIS OF REAL IMAGES

For real night images of different scenes Fig. 3 (a) - (d) show some samples of images that suffer from low light conditions. The results of the corresponding images enhanced using the proposed algorithm are shown in Fig. 3(e) – (h). The proposed algorithm is also compared with other existing algorithms such as P-retinex [9], contrast pair [7], and FB [22] for LLL image in the outdoor scene and the results are displayed in Fig. 4. It is evident that the proposed CED algorithm enhances contrast, removes noise and maintains consistency in colors, while other algorithms improve only the contrast. In the case of contrast pair (Fig. 4 (b)), the human person is not clearly visible, while the image looks unnatural in the case of P-retinex method (Fig. 4(c)) and FB introduces

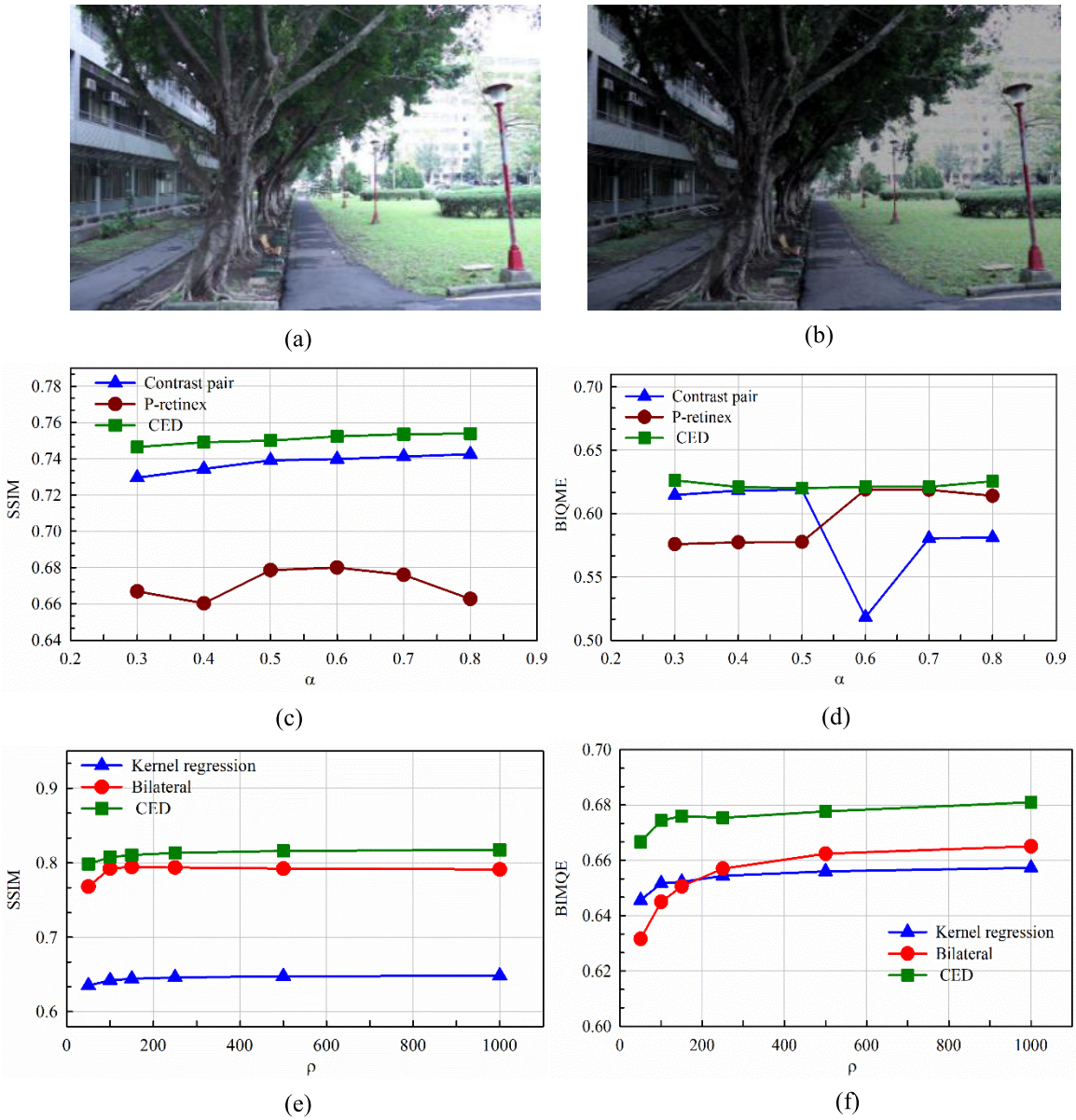

FIGURE 9. Contrast and denoise analysis of various algorithms for simulated image. (a) reference image, (b) example of one simulated image ($\alpha = 0.3$, $\rho = 50$), (c) contrast analysis with FR metric, (d) contrast analysis with blind metric, (e) denoise analysis with FR metric, (f) denoise analysis with blind metric.

checkerboard artifacts in the image as shown in Fig. 4(d). It is encouraging to notice that the CED algorithm avoids over enhancement (Fig. 4 (e)). Therefore, it is obvious that the proposed algorithm achieves better results by preserving the brightness up to the required level without introducing undesirable artifacts.

To substantiate the above results experiments were conducted for more real night images and their results are compared with state-of-the-art low light algorithms. The plots in Fig. 5 (a) and Fig. 5 (b) give the average results of eight (LLL and VLLL) real night images. The results are validated both in terms of blind (NIQMC and BIQME) and FR (SSIM and PSNR) assessment methods. It is evident that the proposed method obtains better results compared with the state-of-the-art algorithms.

To quantify the subjective evaluation of our method, we conducted an independent user study. In this experiment we used different kinds of real night images and enhance them using contrast pair, P-retinex, FB and our proposed method. For each test we randomly order the outputs of the four algorithms and the original image and display them on the screen. We separately asked 25 participants to select the image with best visual quality according to one's perception. From these trails, the percentage of times a viewer selected the output of the proposed method is 60.9%. Input images and three other methods correspond to 0.89%, 10.3%, 12.53%, and 15.32% respectively. This small-scale experiment gives additional support to our conclusion in the qualitative evaluation.

B. SIMULATION MODEL VERIFICATION

Simulation model verification is inevitable to evaluate the effectiveness of the proposed CED algorithm because real night images cannot be used to validate the effectiveness of the proposed algorithm. To verify the simulation model, real and generated night images (from real day image) are compared in Fig. 6. The quality of the images is measured using SSIM and PSNR. The results exhibit that the simulated and real night images have similar appearances. Quantitative analysis reveals that the quality of simulated night image is analogous to real night image. In Fig. 7, simulated night image is used to compare the SSIM outputs of the proposed algorithm with those state-of-the-art techniques such as contrast pair and P-retinex. The effectiveness of the algorithm is evaluated using a simulated image for various levels of contrast with fixed noise $\rho = 3000$ and noise with constant contrast $d = 0.03$; $\alpha = 0.7$. It can be seen from the figure that the proposed method demonstrates the best performance compared with other techniques.

C. PCA ANALYSIS OF REAL IMAGES

PCA analysis with other color transforms is ineluctable as it is indispensable for the proposed work. PCA explores the variance-covariance or correlation structure of samples in vector form. It uncovers the spectral properties of colorants to process the information for better results. Experiments were performed for different color transforms YIQ, HSV, and PCA for ten various types of real images including LLL and VLLL images and the average are calculated. The experimental results of different color transforms are compared and measured with both FR and blind assessment methods where day image is adopted as the reference. Fig. 8 clearly exhibits that PCA obtains better scores that imply better quality of images.

D. CONTRAST ANALYSIS

Contrst enhancement algorithms such as contrast pair and P-retinex are applied to the simulated night images and their result are compared with the proposed algorithm. The source image (Fig. 9(a)) is simulated for various levels of contrast and noise. Fig. 9(b) is the example of one simulated image that is generated with $\alpha = 0.3$, $\rho = 50$. The quantitative results of the algorithm for various levels of contrast and fixed noise are calculated using one FR and blind performance metric as shown in Fig. 9(c) and (d). The results demonstrate that CED-CE (only contrast enhancement) surpass other existing algorithms in terms of contrast and brightness consistently.

E. DENOISE ANALYSIS

Enhancing the contrast amplifies the noise which makes denoising predominant. Poisson noise is inversely proportional to the level of contrast in the night image. The daytime image is used as a reference for quantitative analysis for comparing CED with other denoising algorithms. Poisson noise is random in nature and leads to degradation of image quality and errors. Bilateral filter [37], CED and kernel regression [38] denoising algorithms are applied to the simulated noisy image and their results are compared in Fig. 9(e) and (f). Bilateral filter smoothens the image while preserving the edges. But for high noise levels, the image looks like painting due to smoothing effect. Kernel regression algorithm preserves the details in the image but the noise is still present. However, CED-denoising filter not only removes noise but also preserves the details in the image.

V. CONCLUSION

An effective CED algorithm has been proposed to perform contrast enhancement and denoising for night images. Retinex based adaptive filter is applied in three scales to improve the contrast and brightness significantly. Noise is attenuated through collaborative filtering which reveals even the finest details of the image. The artifacts found in traditional methods are successfully eliminated. Experimental results show that the proposed algorithm can achieve better image quality compared with other state-of-the-art methods. A mathematical model for image degradation is presented to check the effectiveness of the algorithm through simulation. Although the simulated and real night images have similar appearances, the quantitative analysis of simulation model shows that the model can be improved further.

REFERENCES

[1] Z. Ling, Y. Liang, Y. Wang, H. Shen, and X. Lu, "Adaptive extended piecewise histogram equalisation for dark image enhancement," *IET Image Process.*, vol. 9, no. 11, pp. 1012–1019, 2015, doi: 10.1049/iet-ipr.2014.0580.

[2] T. Thaipanich, B. T. Oh, P.-H. Wu, D. Xu, and C.-C. J. Kuo, "Improved image denoising with adaptive nonlocal means (ANL-means) algorithm," *IEEE Trans. Consum. Electron.*, vol. 56, no. 4, pp. 2623–2630, Nov. 2010, doi: 10.1109/TCE.2010.5681149.

[3] M. S. Sayed and D. Justin, "Low complexity contrast enhancement algorithm for nighttime visual surveillance," in *Proc. Int. Conf. Intell. Syst. Design Appl.*, Cairo, Egypt, Nov. 2010, pp. 835–838.

[4] A. Yamasaki, H. Takauji, S. I. Kaneko, T. Kanade, and H. Ohki, "Denighting: Enhancement of nighttime images for a surveillance camera," in *Proc. Int. Conf. Pattern Recognit.*, Tampa, FL, USA, Dec. 2009, pp. 1–4.

[5] L. Li, R. Wang, W. Wang, and W. Gao, "A low light image enhancement method for both denoising and contrast enlarging," in *Proc. IEEE Int. Conf. Image Process.*, Montreal, QC, Canada, Sep. 2015, pp. 3730–3734.

[6] X. Zhang, P. Shen, L. Luo, L. Zhang, and J. Song, "Enhancement and noise reduction of very low light level images," in *Proc. Int. Conf. Pattern Recognit.*, Tsukuba, Japan, Nov. 2012, pp. 2034–2037.

[7] A. R. Rivera, B. Ryu, and O. Chae, "Content-aware dark image enhancement through channel division," *IEEE Trans. Image Process.*, vol. 21, no. 9, pp. 3967–3980, Sep. 2012, doi: 10.1109/TIP.2012.2198667.

[8] Y.-K. Wang and W.-B. Huang, "A CUDA-enabled parallel algorithm for accelerating retinex," *J. Real-Time Image Process.*, vol. 9, no. 3, pp. 407–425, 2014, doi: 10.1007/s11554-012-0301-6.

[9] L. Meylan and S. Susstrunk, "High dynamic range image rendering with a retinex-based adaptive filter," *IEEE Trans. Image Process.*, vol. 15, no. 9, pp. 2820–2830, Sep. 2006, doi: 10.1109/TIP.2006.877312.

[10] E. P. Bennett and L. McMillan, "Video enhancement using per-pixel virtual exposures," in *Proc. ACM SIGGRAPH*, Los Angeles, CA, USA, 2005, pp. 845–852.

[11] M. Kim, D. Park, D. K. Han, and H. Ko, "A novel approach for denoising and enhancement of extremely low-light video," *IEEE Trans. Consum. Electron.*, vol. 61, no. 1, pp. 72–80, Feb. 2015, doi: 10.1109/TCE.2015.7064113.

[12] S. Paris, P. Kornprobst, J. Tumblin, and F. Durand, "Bilateral filtering: Theory and applications," *Found. Trends Comput. Graph. Vis.*, vol. 4, no. 1, pp. 1–73, 2009, doi: 10.1561/0600000020.

[13] W. Dong, L. Zhang, G. Shi, and X. Li, "Nonlocally centralized sparse representation for image restoration," *IEEE Trans. Image Process.*, vol. 22, no. 4, pp. 1620–1630, Apr. 2013, doi: 10.1109/TIP.2012.2235847.
[14] W. Dong, G. Shi, and X. Li, "Nonlocal image restoration with bilateral variance estimation: A low-rank approach," *IEEE Trans. Image Process.*, vol. 22, no. 2, pp. 700–711, Feb. 2013, doi: 10.1109/TIP.2012.2221729.
[15] H. Talebi and P. Milanfar, "Global image denoising," *IEEE Trans. Image Process.*, vol. 23, no. 2, pp. 755–768, Feb. 2014, doi: 10.1109/TIP.2013.2293425.
[16] K. Dabov, A. Foi, V. Katkovnik, and K. Egiazarian, "Color image denoising via sparse 3D collaborative filtering with grouping constraint in luminance-chrominance space," in *Proc. IEEE Int. Conf. Image Process.*, San Antonio, TX, USA, Sep./Oct. 2007, pp. 313–316.
[17] J. Yang, "Enhancement of LLLIs with improved BCP and matrix completion," *Electron. Lett.*, vol. 53, no. 9, pp. 586–588, 2017, doi: 10.1049/el.2016.4686.
[18] Q. Xu, H. Jiang, R. Scopigno, and M. Sbert, "A novel approach for enhancing very dark image sequences," *J. Signal Process.*, vol. 103, pp. 309–330, Oct. 2014, doi: 10.1016/j.sigpro.2014.02.013.
[19] A. Łoza, D. R. Bull, P. R. Hill, and A. M. Achim, "Automatic contrast enhancement of low-light images based on local statistics of wavelet coefficients," *Digit. Signal Process.*, vol. 23, no. 6, pp. 1856–1866, Dec. 2013, doi: 10.1016/j.dsp.2013.06.002.
[20] J. Lim, M. Heo, C. Lee, and C.-S. Kim, "Enhancement of noisy low-light images via structure-texture-noise decomposition," in *Proc. Int. Conf. Signal Inf. Process.*, Jeju, South Korea, Dec. 2016, pp. 1–5.
[21] W. Shi, C. Chen, F. Jiang, D. Zhao, and W. Shen, "Group-based sparse representation for low lighting image enhancement," in *Proc. IEEE Int. Conf. Image Process.*, Phoenix, AZ, USA, Sep. 2016, pp. 4082–4086.
[22] X. Fu, D. Zeng, Y. Huang, Y. Liao, X. Ding, and J. Paisley, "A fusion-based enhancing method for weakly illuminated images," *Signal Process.*, vol. 129, pp. 82–96, Dec. 2016, doi: 10.1016/j.sigpro.2016.05.031.
[23] X. Min, G. Zhai, K. Gu, X. Yang, and X. Guan, "Objective quality evaluation of dehazed images," *IEEE Trans. Intell. Transp. Syst.*, to be published, doi: 10.1109/TITS.2018.2868771.
[24] K. Gu, G. Zhai, X. Yang, W. Zhang, and C. W. Chen, "Automatic contrast enhancement technology with saliency preservation," *IEEE Trans. Circuits Syst. Video Technol.*, vol. 25, no. 9, pp. 1480–1494, Sep. 2015, doi: 10.1109/TCSVT.2014.2372392.
[25] K. Gu, G. Zhai, X. Yang, and W. Zhang, "Hybrid no-reference quality metric for singly and multiply distorted images," *IEEE Trans. Broadcast.*, vol. 60, no. 3, pp. 555–567, Sep. 2014, doi: 10.1109/TBC.2014.2344471.
[26] Z. Wang, A. C. Bovik, H. R. Sheikh, and E. P. Simoncelli, "Image quality assessment: From error visibility to structural similarity," *IEEE Trans. Image Process.*, vol. 13, no. 4, pp. 600–612, Apr. 2004, doi: 10.1109/TIP.2003.819861.
[27] K. Gu, G. T. Zhai, and M. Lin, "The analysis of image contrast: From quality assessment to automatic enhancement," *IEEE Trans. Cybern.*, vol. 46, no. 1, pp. 284–297, Jan. 2015, doi: 10.1109/TCYB.2015.2401732.
[28] X. Min, K. Gu, G. Zhai, J. Liu, X. Yang, and C. W. Chen, "Blind quality assessment based on pseudo-reference image," *IEEE Trans. Multimedia*, vol. 20, no. 8, pp. 2049–2062, Aug. 2018, doi: 10.1109/TMM.2017.2788206.
[29] K. Gu, W. Lin, G. Zhai, X. Yang, W. Zhang, and C. W. Chen, "No-reference quality metric of contrast-distorted images based on information maximization," *IEEE Trans. Cybern.*, vol. 47, no. 12, pp. 4559–4565, Dec. 2017, doi: 10.1109/TCYB.2016.2575544.
[30] K. Gu, D. Tao, J.-F. Qiao, and W. Lin, "Learning a no-reference quality assessment model of enhanced images with big data," *IEEE Trans. Neural Netw. Learn. Syst.*, vol. 29, no. 4, pp. 1301–1313, Apr. 2018, doi: 10.1109/TNNLS.2017.2649101.
[31] X. Min, G. Zhai, K. Gu, Y. Liu, and X. Yang, "Blind image quality estimation via distortion aggravation," *IEEE Trans. Broadcast.*, vol. 64, no. 2, pp. 508–517, Jun. 2018, doi: 10.1109/TBC.2018.2816783.
[32] S. A. Priyanka, H.-J. Tung, and Y. K. Wang, "Contrast enhancement of night images," in *Proc. Int. Conf. Mach. Learn. Cybern.*, Jeju, South Korea, Jul. 2016, pp. 380–385.
[33] D. Y. Tzeng and R. S. Berns, "A review of principal component analysis and its applications to color technology," *Color Res. Appl.*, vol. 30, no. 2, pp. 84–98, Jan. 2005.
[34] M. C. Hanumantharaju, M. Ravishankar, and D. R. Rameshbabu, "Natural color image enhancement based on modified multiscale retinex algorithm and performance evaluation using wavelet energy," in *Recent Advances in Intelligent Informatics*, vol. 235. Springer, 2014, pp. 83–92, doi: 10.1007/978-3-319-01778-5_9.
[35] S.-C. Huang, F.-C. Cheng, and Y.-S. Chiu, "Efficient contrast enhancement using adaptive gamma correction with weighting distribution," *IEEE Trans. Image Process.*, vol. 22, no. 3, pp. 1032–1041, Mar. 2013, doi: 10.1109/TIP.2012.2226047.
[36] R. C. Gonzalez and R. E. Woods, *Digital Image Processing*, 3rd ed. Upper Saddle River, NJ, USA: Prentice-Hall, 2008.
[37] F. Durand and J. Dorsey, "Fast bilateral filtering for the display of high-dynamic-range images," *ACM Trans. Graph.*, vol. 21, no. 3, pp. 257–266, 2002, doi: 10.1145/566654.566574.
[38] H. Takeda, S. Farsiu, and P. Milanfar, "Kernel regression for image processing and reconstruction," *IEEE Trans. Image Process.*, vol. 16, no. 2, pp. 349–366, Feb. 2007, doi: 10.1109/TIP.2006.888330.

STEFFI AGINO PRIYANKA received the bachelor's degree in electronics and communication engineering from the Loyola Institute of Technology, Anna University, India, in 2012, and the master's degree in applied electronics from St. Joseph's College of Engineering, India, in 2014. She is currently pursuing the Ph.D. degree with the Applied Science and Engineering, Fu Jen Catholic University, Taiwan. Her research interests include deep learning, neural networks, computer vision, pattern recognition, and digital image processing.

YUAN-KAI WANG received the B.S. degree in electrical engineering and the Ph.D. degree in computer science and information engineering from National Central University, in 1990 and 1995, respectively. From 1995 to 1999, he was a Post-Doctoral Fellow with the Institute of Information Science, Academia Sinica. In 1999, he joined the Department of Electrical Engineering, Fu Jen Catholic University, as an Associate Professor, where he has been a Professor, since 2017. He was the chair, the co-chair, and the program committee member of many international conferences and a reviewer of many journals and IEEE TRANSACTIONS. He has served in the Board of Directors and Supervisors of the Chinese Image Processing and Pattern Recognition Society, from 2004 to 2010. He has served in the Board of Directors of the Information Service Association of Chinese Colleges, from 2005 to 2007. He was invited as a Panel Speaker for the International Conference of Pattern Recognition, in 2014.

He has published more than 90 papers, with many papers being awarded by conferences as Best Papers, such as the International Conference on Machine Learning and Cybernetics and the International Conference on Pattern Recognition. His research interests include computer vision, pattern recognition, neural networks, genetic algorithms, machine learning, and artificial intelligence, with a special focus on video surveillance, face recognition, biometrics, robotic vision, embedded computer vision, and health care. He was a recipient of the Excellent Research Award of the Ministry of Technology, from 2008 to 2017, the National Industrial Innovation Award, the Excellent Team Award from the National Science Council, in 2011, and the Technology Development Program Paradigm Award from the Ministry of Economic Affairs, in 2012.

SHIH-YU HUANG received the B.S. degree in information engineering from the Tatung Institute of Technology, Taipei, Taiwan, in 1988, and the M.S. and Ph.D. degrees from the Department of Computer Sciences, National Tsing Hua University, Taiwan, in 1990 and 1995, respectively. From 1995 to 1999, he was with the Telecommunication laboratory, Chungwa Telecom Co., Ltd., Taiwan. In 1999, he joined the Department of Computer Science and Information Engineering, Ming Chuan University, Taiwan. His current research interests are video processing and steganography.